Collisional Damping of Electron Bernstein Waves and its Mitigation by Evaporated Lithium Conditioning in Spherical-Tokamak Plasmas

S. J. Diem,[1] G. Taylor,[2] J. B. Caughman,[1] P. C. Efthimion,[2] H. Kugel,[2] B. P. LeBlanc,[2] C. K. Phillips,[2] J. Preinhaelter,[3] S. A. Sabbagh,[4] and J. Urban[3]

[1]*Oak Ridge National Laboratory, Oak Ridge 37831, Tennessee, USA*
[2]*Princeton Plasma Physics Laboratory, Princeton, New Jersey 08543, USA*
[3]*EURATOM/IPP.CR Association, Institute of Plasma Physics, 18200 Prague 8, Czech Republic*
[4]*Columbia University, New York, New York 10027, USA*

(Received 28 October 2008; published 30 June 2009)

The first experimental verification of electron Bernstein wave (EBW) collisional damping, and its mitigation by evaporated Li conditioning, in an overdense spherical-tokamak plasma has been observed in the National Spherical Torus Experiment (NSTX). Initial measurements of EBW emission, coupled from NSTX plasmas via double-mode conversion to O-mode waves, exhibited $<10\%$ transmission efficiencies. Simulations show 80% of the EBW energy is dissipated by collisions in the edge plasma. Li conditioning reduced the edge collision frequency by a factor of 3 and increased the fundamental EBW transmission to 60%.

DOI: 10.1103/PhysRevLett.103.015002 PACS numbers: 52.35.Hr, 52.35.Fp, 52.35.Mw, 52.35.Qz

Electrostatic electron Bernstein wave (EBW) mode conversion (MC) to electromagnetic waves has been of interest to a wide variety of physics subfields, including astrophysics [1–5], semiconductor physics [6,7], laser-produced [8,9], and magnetically confined plasmas [10,11]. EBWs propagate perpendicular to the magnetic field in hot, overdense plasmas (where $\omega_{pe} \gg \Omega_{ce}$, ω_{pe} is the electron plasma frequency and Ω_{ce} is the electron cyclotron frequency), are readily absorbed and emitted from electron cyclotron (EC) resonance locations and do not experience a high density cutoff. Recently, there has been an increased interest in EBW heating (EBWH) and current drive (EBWCD) in overdense, magnetically confined, plasma devices, such as the spherical tokamak (ST) and the reverse field pinch (RFP), where the standard techniques of electron cyclotron resonance heating (ECRH) and current drive (ECCD) [12] cannot be used.

EBWs exist only in the overdense regime but can be excited from outside the plasma via double MC from the ordinary mode electron cyclotron wave and then to the slow extraordinary mode (O-X-B) [13–15]. O-X-B heating was first successfully demonstrated on the W7-AS stellarator [10], and more recently on the Mega-Amp Spherical Torus (MAST) [11].

The physics of EBW emission (EBE), via B-X-O MC, is essentially the reverse process to the O-X-B MC used for heating [16], except that the introduction of RF power may excite lossy nonlinear phenomena, like parametric decay [17,18]. This Letter reports the results from studying B-X-O emission from the National Spherical Tokamak Experiment (NSTX) [19]. NSTX operates with plasmas that have relatively high electron densities, $n_e = 10^{19}$–10^{20} m^{-3}, and low magnetic fields on axis, $B_t(0) < 0.6$ T, so that up to the fourth EC harmonic resonance is overdense. A critical challenge is to demonstrate that efficient EBW coupling can be sustained in High confinement mode (H mode, which is characterized by a steep edge density gradient), ST plasmas in order for EBWCD to be viable in this role.

Previous simulations of EBE in NSTX [20,21] predicted that strong collisional damping of EBWs prior to conversion to the slow X mode [22] occurs when $\nu_{ei}/\omega > 10^{-4}$ (where ν_{ei} is the electron-ion collision frequency and ω is the wave frequency) near the MC layer and that this can significantly reduce the observed EBE levels. In this Letter, the first experimental observation and control of EBW collisional damping in the plasma edge during H-mode operation is presented. The effects of EBW collisional damping were significantly decreased when evaporated lithium edge conditioning depleted the electron density in the edge plasma, thereby moving the MC layer to a region near the last closed flux surface (LCFS) where $\nu_{ei}/\omega < 10^{-4}$ (or typically where $T_e > 20$ eV in NSTX).

EBE measurements presented in this Letter are acquired with a remotely steered quad-ridged microwave antenna measuring fundamental, second, and third harmonic (18–36 GHz) emission. The antenna is mounted outside of the vacuum vessel and coupled to an absolutely calibrated heterodyne radiometer system [23,24]. The antenna beam waist diameter is 13 cm at the LCFS, which is located 50 cm from the antenna. In NSTX, the optical thickness, τ, is $\sim$3000 [25], easily satisfying the blackbody emission condition of $\tau > 2$. Therefore, the measured radiation temperature, T_{rad}, is assumed to be blackbody radiation and equal to the local electron temperature, T_e, provided the B-X-O transmission efficiency is $\sim$100%.

The measured emission is simulated with a numerical EBE simulation code [26]. The code launches 41 rays to model the antenna pattern of the EBE diagnostic. A full-wave code is used to calculate the efficiency of the O-X-B

mode conversion process while a 3D ray-tracing calculation describes the EBW propagation into the plasma until it is damped near the EC resonance layer. Since the physics of launched *O-X-B* power is the reverse process of *B-X-O* emission, neglecting any parasitic effects, the results from the EBE simulations can be directly compared to EBE measurements. Collisions are incorporated into the code with a Bhatnagar-Gross-Krook collision operator [27,28]. The effect of electron-electron collisions are neglected due to conservation of momentum while electron-neutral collisions are ignored because the neutral density is less than 5% of the electron density near the MC layer. Therefore, only the effects of electron-ion collisions are incorporated in the EBE simulation code. The code uses the T_e and n_e profiles from laser Thomson scattering [29], EFIT magnetic equilibria [30], and the experimentally measured antenna pattern.

Initial EBE measurements of *H*-mode plasmas (I_p = 1 MA, $n_e(0) = 3\text{–}6 \times 10^{19}\ \mathrm{m}^{-3}$, $T_e(0) = 0.9$ keV, $B_t(0) =$ 4 kG) in NSTX exhibited a period of strong emission before the low-confinement mode (referred to as *L* mode, this is the first phase of the plasma discharge and is characterized by a shallow edge density gradient) to *H*-mode transition (*L-H*) followed by a rapid decay of emission. The decay was observed for emission from all measured EC harmonics. The EBW emission location remained at the same major radius location during the discharge. An example of this behavior is shown in Fig. 1. Figure 1(a) shows the time evolution of $T_e(0)$ and the calculated *B-X-O* transmission efficiency for a plasma with an *H*-mode transition at 0.17 s. The *B-X-O* transmission efficiency is calculated by taking the ratio of the measured T_{rad} to measured T_e (from laser Thomson scattering) at the simulated EBW emission location. The time evolution of the measured T_{rad} for second harmonic EBE at 24 GHz emitted from a major radius of 1 m for this shot is shown in the bottom solid line in Fig. 1(b). An EBE simulation of second harmonic emission at 24 GHz without collisional damping effects [Fig. 1(b)] predicts that T_{rad} is a factor of 4 above the measured value. When collisional damping effects are included in the simulations by using a measured effective ion charge state, Z_{eff}, of 2, the simulated EBE T_{rad} decays soon after the *H*-mode transition [Fig. 1(b)]. The Z_{eff} is measured 5 cm inboard from the MC layer, where simulations predict >90% of the EBW collisional damping occurs. It is calculated based upon measuring the line emission from plasmas where the sole impurity is carbon; however, with other impurities present the Z_{eff} value can be higher. EBE simulations with Z_{eff} of 3–4 agree much closer with the measured results as shown in Fig. 1(b).

For times >0.25 s, the MC layer location is shifted outside the LCFS and the peak ratio of ν_{ei}/ω increased by over a factor of 2 from 5×10^{-5} at $t = 0.148$ s to 1.25×10^{-4} at $t = 0.348$ s [Fig. 2(a)]. Subsequently, T_e at the MC layer decreased from 30 eV to <10 eV during

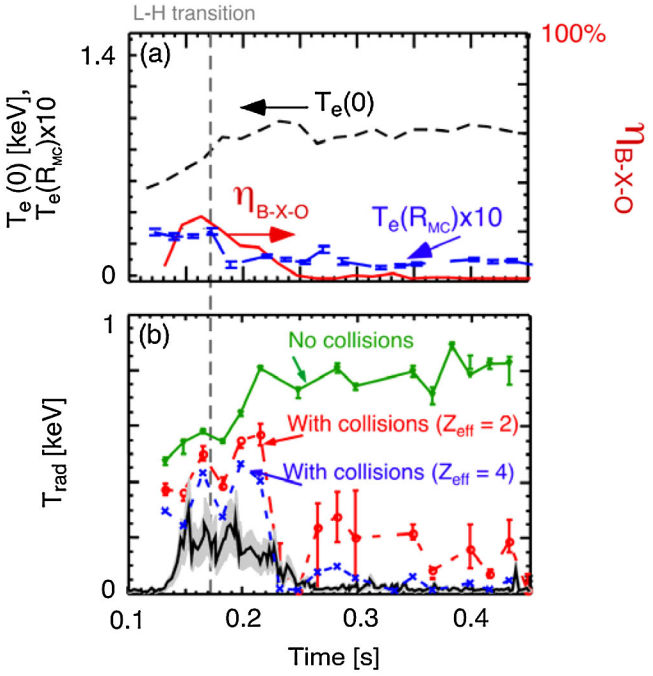

FIG. 1 (color online). (a) The central T_e (dashed line), T_e at the MC layer (dashed line with error bars indicating error in laser Thomson scattering measurement) and *B-X-O* transmission efficiency (solid line) are plotted as a function of time. The vertical dashed line indicates the time of the *L-H* transition. (b) The solid line indicates the measured T_{rad} (second harmonic EBE at 24 GHz) for an *H*-mode plasma. The EBE simulated T_{rad} without (bottom solid line) and with (long dashed line for $Z_{\mathrm{eff}} =$ 2 and short dashed line for $Z_{\mathrm{eff}} = 4$) collisional damping effects are shown as a function of time. The shaded grey region indicates the uncertainty in the measured T_{rad}. The error bars for the EBE simulations include the error in the n_e and T_e measurements as well as the magnetic equilibria.

the *L-H* mode transition [Fig. 1(a)]. Simulations show that EBWs are strongly damped for values of $\nu_{\mathrm{ei}}/\omega > 10^{-4}$. Additionally, simulations predict that 20%–40% of the ray intensity is collisionally damped prior to $t = 0.25$ s, while 70%–90% is collisionally damped after $t = 0.25$ s [Fig. 2(b)]. These results suggest that a significant fraction of injected power may collisionally damp shortly after *O-X-B* conversion in this *H*-mode plasma.

These *H*-mode EBE measurements indicate that in order to increase the *B-X-O* transmission efficiency, and in turn the *O-X-B* transmission, it is necessary to reduce the collisionality near the MC layer. A tool that is available to NSTX for edge conditioning is the LIThium EvaporatoR (LITER) [31]. LITER creates a solid lithium coating on the centerstack and lower divertor that pumps D^+ and D^0 by forming LiD. Lithium pumping can lead to a decrease in the edge electron density that can move the MC layer to regions of increased T_e and lower collisionality.

In a sequence of similar *H*-mode plasmas ($I_p =$ 0.8 MA, $n_e(0) \sim 3 \times 10^{19}\ \mathrm{m}^{-3}$, $T_e(0) \sim 0.8$ keV, $B_t =$ 4.5 kG), the lithium evaporation rate was increased from 0 to 19 mg/min in order to scan the collisionality at the

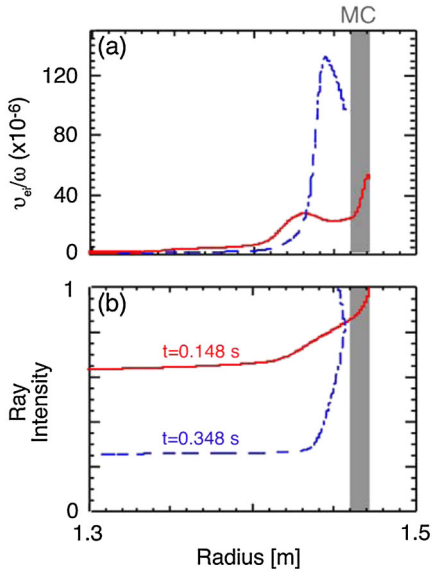

FIG. 2 (color online). Comparison of (a) υ_{ei}/ω and (b) ray intensity as a function of major radius for two time points: $t = 0.148$ s, during high emission (solid line), and $t = 0.348$ s, after the decay of EBE (dashed line). The grey region indicates the location of the MC layer.

MC layer. As a result of Li edge conditioning, n_e in the plasma edge was reduced by nearly a factor of 2 and, consequently, the MC layer moved from several cm outside the LCFS to near the plasma separatrix [Fig. 3(a)]. By moving the MC layer closer to the plasma, T_e at the fundamental MC layer during the H-mode phase increased from 5–9 eV (no Li) to nearly 20 eV (with Li) as shown in Fig. 3(b). The emission antenna had a fixed, oblique view of the plasma to obtain the results shown in this scan. Emission at 18 GHz, corresponding to fundamental EBE from near the plasma axis at a major radius of 1 m, increased from $T_{\mathrm{rad}} \sim 50$ eV to $T_{\mathrm{rad}} \sim 450$ eV during the lithium evaporation scan [Fig. 4(b)]. The central T_e increased by only 10% [Fig. 4(a)] during the scan, so this does not account for the observed nearly order of magnitude increase in the measured T_{rad}. The calculated B-X-O transmission efficiency for fundamental emission at 18 GHz during the edge collisionality scan is shown in Fig. 4(c). With lithium edge conditioning, the calculated transmission efficiency was observed to increase from 10% to 60%.

A significant decrease in the calculated edge collisionality occurred with the increase in the lithium evaporation rate [Fig. 5(a)]. With no lithium conditioning, simulations predict that υ_{ei}/ω within 5 cm of the MC layer peaked

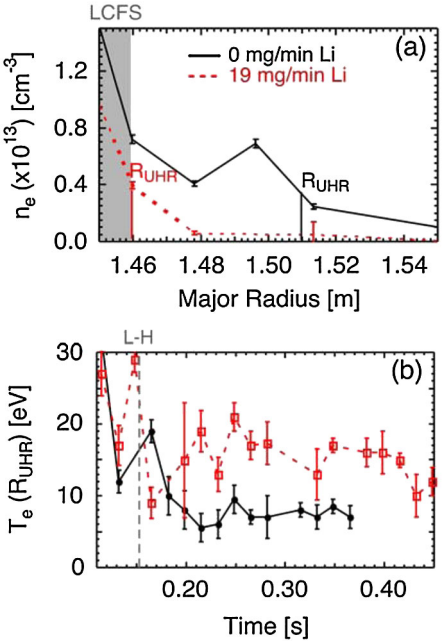

FIG. 3 (color online). The (a) edge density and (b) electron temperature at the UHR layer are shown as a function of time for a plasma without Li conditioning (solid line) and a case with Li conditioning (dashed line). Error bars are indicated by the vertical lines.

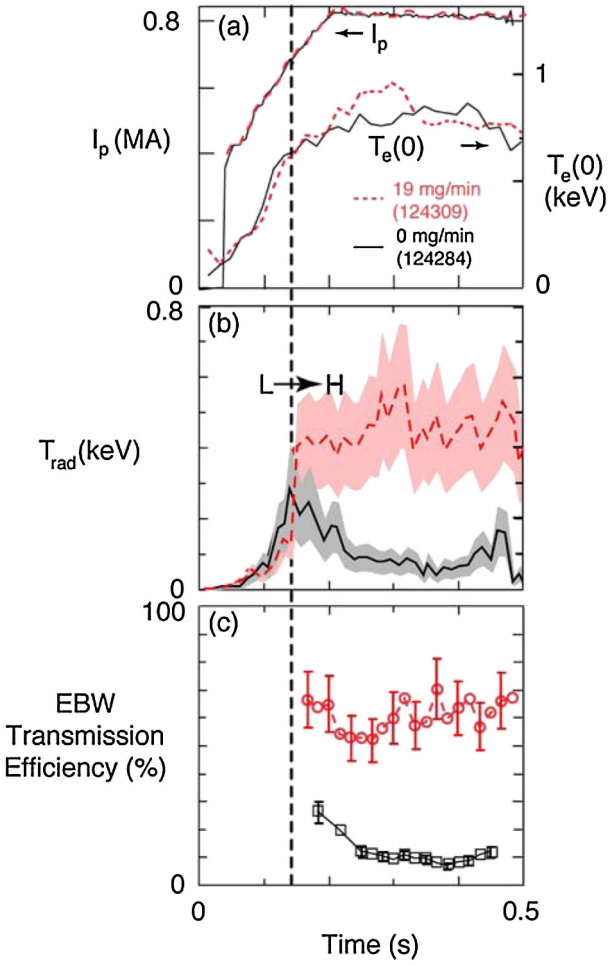

FIG. 4 (color online). (a) The plasma current, I_p, and central T_e are plotted as a function of time for an H-mode plasma. The measured (b) T_{rad} and (c) B-X-O transmission efficiency as a function of time are plotted for 0 mg/min (solid line) and 19 mg/min = 286 total mg of evaporated lithium (dashed line).

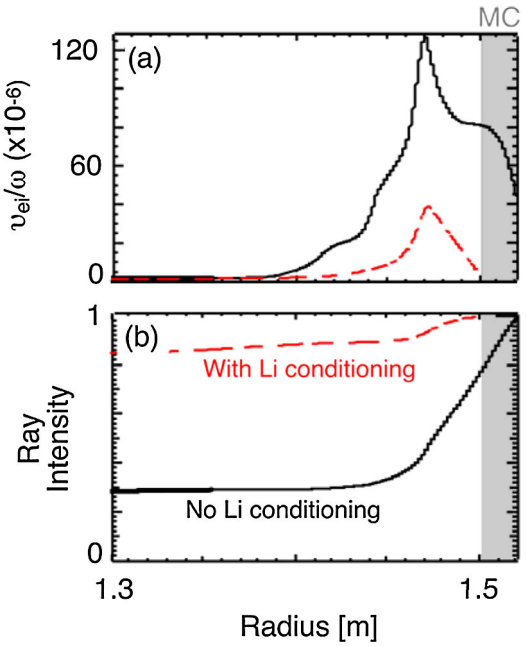

FIG. 5 (color online). Comparison of (a) υ_{ei}/ω and (b) ray intensity as a function of major radius for two cases: without lithium conditioning (dashed line) and with lithium conditioning (solid line). The grey region indicates the location of the MC layer.

at 12×10^{-5}. By increasing the lithium evaporation rate to 19 mg/min, υ_{ei}/ω within 5 cm of the MC layer calculated by the EBE simulation decreased by over a factor of 3 to 4×10^{-5}. The EBE simulation results still show a significant reduction of υ_{ei}/ω even though the edge Z_{eff} increases from 1.5 to 2.5 during the scan. Consequently, simulations show that the fraction of power in the EBW branch that is lost to collisional damping decreased from nearly 70% to only 15% with the application of 19 mg/min of edge lithium conditioning [Fig. 5(b)].

In conclusion, the first observation of EBW collisional damping during the *B-X-O* mode conversion process, and its mitigation by lithium evaporation, has been made in NSTX. Initial EBE measurements and simulations of second harmonic emission at 24 GHz indicate that nearly 80% of the EBE intensity was absorbed in the plasma edge prior to mode conversion to the *X* and *O* modes. Edge lithium conditioning was successfully used to decrease n_e in the edge plasma, moving the MC layer into a region with reduced collisionality. Simulations have shown that EBE intensity increased from 30% to 85% with edge conditioning. The measured *B-X-O* transmission efficiency increased from 10% to 60% by reducing the EBW collisional damping losses. An increase in the measured T_{rad} from ~50 eV to >450 eV was also observed.

The results of this Letter suggest that future EBW heating or current drive experiments involving *H*-mode ST plasmas may suffer from EBW collisional damping effects when $\upsilon_{ei}/\omega > 10^{-4}$ inside the EBW MC layer. Edge conditioning methods may be implemented to reduce the effects of EBW collisional damping, allowing efficient rf power coupling to the plasma.

This research is supported by U.S. Department of Energy Grant No. DE-AC02-76CH03073, No. DE-FG02-91ER-54109, No. DE-FG03-02ER54684, No. DE-FG02-99ER-54521 and a grant to encourage innovations in fusion diagnostic systems and Grant No. 202/08/0419 of The Czech Science Foundation.

[1] Bernhardt *et al.*, Phys. Rev. Lett. **72**, 2879 (1994).
[2] T. B. Lesser *et al.*, Phys. Rev. Lett. **63**, 1145 (1989).
[3] P. Stubbe and H. Kopka, Phys. Rev. Lett. **65**, 183 (1990).
[4] Leyser *et al.*, Phys. Rev. Lett. **68**, 3299 (1992).
[5] Thide *et al.*, Phys. Rev. Lett. **49**, 1561 (1982).
[6] C. K. N. Patel and R. E. Slusher, Phys. Rev. Lett. **21**, 1563 (1968).
[7] R. E. Slusher *et al.*, Phys. Rev. Lett. **18**, 227 (1967).
[8] C. Grebogi *et al.*, Phys. Rev. Lett. **39**, 338 (1977).
[9] W. Woo *et al.*, Phys. Rev. Lett. **21**, 1419 (1968).
[10] H. P. Laqua *et al.*, Phys. Rev. Lett. **78**, 3467 (1997).
[11] V. Shevchenko *et al.*, Fusion Sci. Technol. **52**, 202 (2007).
[12] H. Zohm, Fusion Sci. Technol. **52**, 134 (2007).
[13] J. Preinhaelter and V. Kopecky, J. Plasma Phys. **10**, 1 (1973).
[14] E. Mjølhus, J. Plasma Phys. **31**, 7 (1984).
[15] F. R. Hansen *et al.*, J. Plasma Phys. **39**, 319 (1988).
[16] A. K. Ram, A. Bers, and C. N. Lashmore-Davies, Phys. Plasmas **9**, 409 (2002).
[17] Ya. N. Istomin and T. B. Leyser, Phys. Plasmas **2**, 2084 (1995).
[18] V. K. Yadav and D. Bora, Phys. Plasmas **11**, 3409 (2004).
[19] M. Ono *et al.*, Nucl. Fusion **40**, 557 (2000).
[20] J. Preinhaelter *et al.*, Rev. Sci. Instrum. **77**, 10F524 (2006).
[21] J. Urban *et al.*, Bull. Am. Phys. Soc. **52**, 304, Paper TP8 104 (2007).
[22] S. Pesic, Physica (Amsterdam) **125B**, 118 (1984).
[23] S. J. Diem *et al.*, Rev. Sci. Instrum. **77**, 10E919 (2006).
[24] S. J. Diem *et al.*, Rev. Sci. Instrum. **79**, 10F101 (2008).
[25] P. C. Efthimion *et al.*, Rev. Sci. Instrum. **70**, 1018 (1999).
[26] J. Urban and J. Preinhaelter, J. Plasma Phys. **72**, 1041 (2006).
[27] P. L. Bhatnagar, E. P. Gross, and M. Krook, Phys. Rev. **94**, 511 (1954).
[28] E. P. Gross and M. Krook, Phys. Rev. **102**, 593 (1956).
[29] B. P. Leblanc *et al.*, Rev. Sci. Instrum. **74**, 1659 (2003).
[30] L. Lao *et al.*, Nucl. Fusion **25**, 1611 (1985).
[31] H. Kugel *et al.*, J. Nucl. Mater. **363–365**, 791 (2007).